

## Dark Matter Annihilation in the Milky Way Galaxy: Effects of Baryonic Compression

F. Prada,<sup>1</sup> A. Klypin,<sup>2</sup> J. Flix,<sup>3</sup> M. Martínez,<sup>3</sup> and E. Simonneau<sup>4</sup>

<sup>1</sup>Ramón y Cajal Fellow, Instituto de Astrofísica de Andalucía (CSIC), E-18008 Granada, Spain

<sup>2</sup>Department of Astronomy, New Mexico State University, Las Cruces New Mexico 88003-8001, USA

<sup>3</sup>Institut de Física D'Altes Energies, Universitat Autònoma, E-08193 Barcelona, Spain

<sup>4</sup>Institut d'Astrophysique de Paris, CNRS, 75014 Paris, France

(Received 23 January 2004; revised manuscript received 26 October 2004; published 7 December 2004)

If the dark matter (DM), which is considered to constitute most of the mass of galaxies, is made of supersymmetric particles, the central region of our Galaxy should emit  $\gamma$  rays produced by their annihilation. We use detailed models of the Milky Way to make accurate estimates of continuum  $\gamma$ -ray fluxes. We argue that the most important effect, which was previously neglected, is the compression of the dark matter due to the infall of baryons to the galactic center: it boosts the expected signal by a factor 1000. To illustrate this effect, we computed the expected  $\gamma$  fluxes in the minimal supergravity scenario. Our models predict that the signal could be detected at high confidence levels by imaging atmospheric Čerenkov telescopes assuming that neutralinos make up most of the DM in the Universe.

DOI: 10.1103/PhysRevLett.93.241301

PACS numbers: 95.35.+d, 14.80.Ly, 98.35.Gi

There is an increasing hope that the new generation of imaging atmospheric Čerenkov telescopes (IACT) will detect in the near future the  $\gamma$  rays coming from the annihilation products of the supersymmetric (SUSY) dark matter (DM) in galaxy halos (e.g., [1–3]). The success of such a detection will solve one of the most fundamental questions in physics: the nature of the dark matter. The lightest SUSY particle (LSP) has been proposed to be a suitable candidate for the nonbaryonic cold DM (e.g., [4]). The LSP is stable in SUSY models where  $R$  parity is conserved [5,6] and its annihilation cross section and mass leads appropriate relic densities [7] in the range allowed by the Wilkinson Microwave Anisotropy Probe (WMAP), i.e.,  $0.095 < \Omega_{\text{CDM}} h^2 < 0.129$  [8]. Most of SUSY breaking scenarios yields the lightest neutralino ( $\tilde{\chi}_1^0$ ) as the leading candidate for the cold DM. The  $\tilde{\chi}_1^0$  remains undiscovered, but a lower mass limit of  $\sim 40$  GeV is already available from accelerators constrains [9]. The  $\tilde{\chi}_1^0$  may annihilate producing  $\gamma$  rays, among other final states.

The number of  $\tilde{\chi}_1^0$  annihilations in galaxy halos and therefore the expected  $\gamma$  signal arriving at the Earth depends not only on the adopted SUSY model but also strongly depends on the DM density  $\rho_{\text{dm}}(r)$ . This is why the central region  $r < 200$  pc of the Milky Way (MW), where the density is the largest, is the favorite site to search for this signal. The expected total number of continuum  $\gamma$ -ray photons received per unit time and per unit area, from a circular aperture on the sky of width  $\sigma_t$  (the resolution of the telescope) observing at a given direction  $\Psi_0$  relative to the center of the MW can be written as

$$F(E > E_{\text{th}}) = \frac{1}{4\pi} f_{\text{SUSY}} U(\Psi_0), \quad f_{\text{SUSY}} = \frac{N_\gamma \langle \sigma v \rangle}{2m_\chi^2},$$

$$U(\Psi_0) = \int J(\Psi) B(\Omega) d\Omega. \quad (1)$$

The factor  $f_{\text{SUSY}}/4\pi$  represents the isotropic probability of  $\gamma$ -ray production per unit of DM density and depends only on the physics of annihilating  $\tilde{\chi}_1^0$  particles. It can be determined for any SUSY scenario given the  $\tilde{\chi}_1^0$  mass  $m_\chi$ , the number of continuum  $\gamma$ -ray photons  $N_\gamma$  emitted per annihilation, with energy above the IACT energy threshold ( $E_{\text{th}}$ ), and the thermally average cross section  $\langle \sigma v \rangle$ .

All the astrophysical properties (such as the DM distribution and geometry considerations) appear only in the factor  $U(\Psi_0)$ . This factor also accounts for the beam smearing, where  $J(\Psi) = \int_{\text{l.o.s.}} \rho_{\text{dm}}^2(r) dl$ ,  $dl = \pm r dr / \sqrt{r^2 - d_\odot^2 \sin^2 \Psi}$ , is the integral of the square of the DM density along the direction  $\Psi$ , and  $B(\Omega) d\Omega$  is the Gaussian beam of the telescope:

$$B(\Omega) d\Omega = \exp\left[-\frac{\theta^2}{2\sigma_t^2}\right] \sin\theta d\theta d\varphi. \quad (2)$$

The angles  $\theta$  and  $\varphi$  are related with the direction of observation  $\Psi_0$  and the line-of-sight angle  $\Psi$  by  $\cos\Psi = \cos\Psi_0 \cos\theta + \sin\Psi_0 \sin\theta \cos\varphi$ . The observer is located in the galactic equatorial plane at a distance  $d_\odot$  (here 8.0 kpc).

A cuspy DM halo  $\rho_{\text{dm}}(r) \propto r^{-\alpha}$  predicted by the simulations of the cold dark matter with the cosmological constant ( $\Lambda$ CDM) is often assumed for the calculations of  $U(\Psi_0)$  (e.g., [1–3,10–12], and references therein). Cosmological  $N$ -body simulations indicate that the distribution of DM in relaxed halos varies between two shapes: the Navarro-Frenk-White (NFW) [13] density profile with asymptotic slope  $\alpha = 1$  and the steeper Moore *et al.* [14] profile with slope 1.5. The most recent numerical models indicate that the central slope is shallower than 1.5. We consider Moore *et al.* profile as a somewhat unrealistic upper limit on uncompressed DM density. Profiles shallower than NFW are sometimes dis-

cussed, but as far as we know, those are typically extrapolations: no real high resolution simulation actually have shown a core [15–17].

*Milky Way mass models with adiabatic compression.*—The predictions for the DM halos are valid *only* for halos without baryons. When normal gas (“baryons”) loses its energy through radiative processes, it falls to the central region of forming galaxy. As the result of this redistribution of mass, the gravitational potential in the center changes substantially. The DM must react to this deeper potential by moving closer to the center and increasing its density. This increase in the DM density is often treated using adiabatic invariants. This is justified because there is a limit to the time scale of changes in the mass distribution: changes of the potential at a given radius cannot happen faster than the dynamical time scale defined by the mass inside the radius. Adiabatic contraction of dark matter in a collapsing protogalaxy was used already in 1962 [18]. In 1980, Zeldovich *et al.* [19] used it to set constraints of properties of elementary particles (annihilating massive neutrinos). The present form of analytical approximation (circular orbits) was introduced in [20]. If  $M_{\text{in}}(r_{\text{in}})$  is the initial distribution of mass (the one predicted by cosmological simulations), then the final (after compression and formation of galaxy) mass distribution is given by  $M_{\text{fin}}(r)r = M_{\text{in}}(r_{\text{in}})r_{\text{in}}$ , where  $M_{\text{fin}} = M_{\text{DM}} + M_{\text{bar}}$ . This approximation was tested in numerical simulations [21,22]. The approximation assumes that orbits are circular, and thus  $M(r)$  is the mass inside the orbit. This is not true for elongated orbits: mass  $M(r)$  is smaller than the real mass, which a particle “feels” when it travels along elongated trajectory. This difference in masses requires a relatively small correction: mass  $M$  should be replaced by the mass inside time-averaged radius of trajectories passing through given radius  $r$ :  $M_{\text{fin}}(\langle r \rangle)r = M_{\text{in}}(\langle r_{\text{in}} \rangle)r_{\text{in}}$ . We find the correction using Monte Carlo realizations of trajectories in the NFW equilibrium halo and finding the time-averaged radii  $\langle x \rangle \approx 1.72x^{0.82}/(1 + 5x)^{0.085}$ ,  $x \equiv r/r_s$ . This approximation predicts a factor of

2 smaller contraction in the central regions, where individual trajectories are very elongated. It gives better fits when compared with realistic cosmological simulations [22].

In order to make realistic predictions for annihilation rates, we construct two detailed models of the MW Galaxy by redoing the full analysis of numerous observational data collected in [23]. The models are compatible with the available observational data for the MW and their main parameters are given in Table I. Models assume that without cooling the density of baryons is proportional to that of the DM and the final baryon distribution is constrained by the observational data. Figure 1 presents the distribution of mass and density in the models. While all observations were included, some of them are more important than others. The solar neighborhood is relatively well studied and, thus, provides important observational constraints. In Table I we present two local parameters: the total density of matter inside 1.1 kpc  $\Sigma_{\text{total}}$  (obtained from kinematics of stars) and the surface density of gas and stellar components  $\Sigma_{\text{baryon}}$ . Circular velocity  $V_{\text{circ}}$  at 3 kpc distance from the center provides another crucial constraint on models as emphasized in [24]. It is difficult to estimate errors of this parameter because of uncertain contribution of the galactic bar. We use  $\pm 5$  km/s error, which is realistic, but it can be even twice larger. Probably the most debated constraint is coming from counts of microlensing events in the direction of the galactic bulge. Our models are expected to have the optical depth of microlensing events  $\tau = 1.2\text{--}1.6 \times 10^{-6}$  and, thus, they are compatible with the values of  $\tau$  determined recently from the observations  $\tau = 1\text{--}1.5 \times 10^{-6}$  [25], but are excluded if  $\tau > 2 \times 10^{-6}$  (see [23] for a detailed discussion on the bulge optical depth in our models).

*Computation of  $f_{\text{SUSY}}$  in the MSUGRA scenario.*—To illustrate the expected variations of  $f_{\text{SUSY}}$  we focus on the minimal supergravity (MSUGRA) scenario. We are using the *Darksusy* package [26] to compute  $\tilde{\chi}_1^0$  relic densities

TABLE I. Models and constraints for the Milky Way Galaxy.

|  | Model A<br>NFW | Model B<br>Moore <i>et al.</i> | Constr.                      |
|--|----------------|--------------------------------|------------------------------|
| Virial mass, $10^{12}M_{\odot}$  | 1.07           | 1.14                           |                              |
| Virial radius, kpc   | 264            | 270                            |                              |
| Halo concentration C   | 11             | 12                             | 10.3–21.5<br>( $1.5\sigma$ ) |
| Disk mass, $10^{10}M_{\odot}$  | 3.7            | 4.0                            |                              |
| Disk scale length, kpc   | 3.2            | 3.5                            | 2.5–3.5                      |
| Bulge mass, $10^9M_{\odot}$  | 8.0            | 8.0                            |                              |
| Black hole mass, $10^6M_{\odot}$   | 2.6            | 2.6                            | 2.6                          |
| $M(<100 \text{ kpc})$ , $10^{11}M_{\odot}$   | 6.25           | 5.8                            | $7.5 \pm 2.5$                |
| $\Sigma_{\text{total}}$ , $ z  < 1.1 \text{ kpc}$ at $R_{\odot}$ , $M_{\odot}\text{pc}^{-2}$ | 65             | 70                             | $71 \pm 6$                   |
| $\Sigma_{\text{baryon}}$ at $R_{\odot}$ , $M_{\odot}\text{pc}^{-2}$                          | 47             | 53                             | $48 \pm 8$                   |
| $V_{\text{circ}}$ at 3 kpc, km/s   | 203            | 205                            | $200 \pm 5$                  |

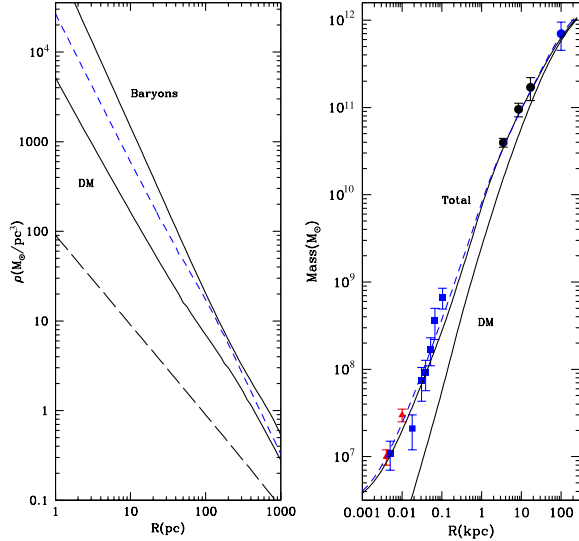


FIG. 1 (color online). Left: the top curve is the density of baryons. The dashed and full curves “DM” are for the compressed Moore *et al.* and NFW models. The long-dashed curve is the uncompressed NFW profile. Right: The solid and dashed curves are the total mass in compressed NFW and Moore *et al.* models. DM mass in the NFW model is the thick curve. Symbols show observational constraints as taken from Klypin *et al.* [23].

and annihilation properties for  $10^6$  MSUGRA random models. We also check that results are not ruled out by present accelerator bounds. In Fig. 2 we show the result of the scan, which covers the relevant regimes in MSUGRA parameter space [27]. All models within WMAP allowed relic densities leads to  $\tilde{\chi}_1^0$  masses from 70 up to 1400 GeV, approximately. The  $\langle\sigma v\rangle$  lies in the range  $1 \times 10^{-29}$  to  $3 \times 10^{-26} \text{ cm}^{-3} \text{ s}^{-1}$ . We also compute the  $f_{\text{SUSY}}/10^{-32}$  dependence with the IACT  $E_{\text{th}}$ . For a given  $E_{\text{th}}$ , the shadow region scans all the  $m_\chi$ ,  $\langle\sigma v\rangle$ , and  $N_\gamma$  intervals. This gives the allowed  $f_{\text{SUSY}}$  region for  $\tilde{\chi}_1^0$  which can be detected with the IACT, i.e., those with  $m_\chi \geq E_{\text{th}}$ .

A complete analysis of all different SUSY scenarios is well above the scope of this letter. We left our further results as a function of factor  $f_{\text{SUSY}}$ , as other SUSY scenarios may give different results on the factor  $f_{\text{SUSY}}$  and upper mass limits.

*Gamma-ray annihilation observability in the Milky Way.*—The expected  $\tilde{\chi}_1^0$  annihilation  $\gamma$  flux can be computed from Eq. (1) for the compressed DM density profile provided by our MW models as a function of the angular distance  $\Psi_0$  from the galactic center. In Fig. 3 we show the predicted fluxes in units of  $f_{\text{YUSY}}/10^{-32}$ . We also show as a comparison the expected flux for the uncompressed NFW density profile. The flux profiles were determined for a typical IACT of resolution  $\sigma_t = 0.1^\circ$  ( $\Delta\Omega = 10^{-5} \text{ sr}$ ). We have multiplied the flux profiles by a factor of 1.7 quoted by Stoehr *et al.* [3] to account for the presence of substructure inside the MW halo [28].

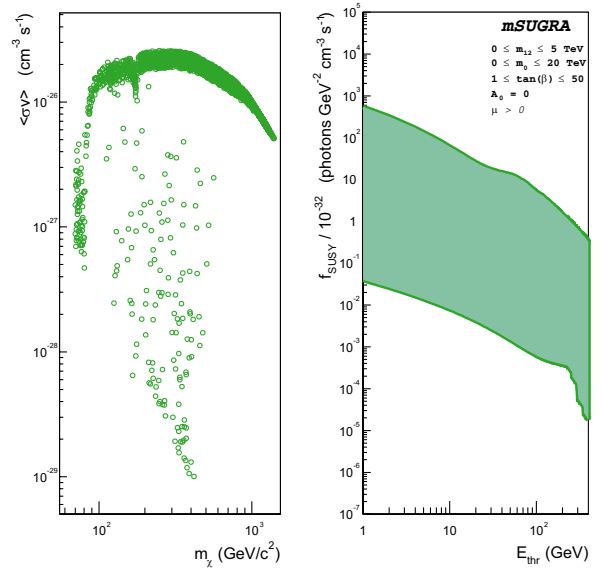


FIG. 2 (color online). Allowed WMAP  $\tilde{\chi}_1^0$  annihilation  $\langle\sigma v\rangle$  and  $f_{\text{SUSY}}$  in the scanned MSUGRA scenario.

The success of a detection requires that the minimum detectable  $\gamma$  flux  $F_{\text{min}}$  for an exposure of  $t$  seconds, given an IACT of effective area  $A_{\text{eff}}$ , angular resolution  $\sigma_t$  and threshold energy  $E_{\text{th}}$  exceeds a significant number  $M_s$  of standard deviations ( $M_s \sigma$ ) the background noise  $\sqrt{N_b}$ , i.e.,  $F_{\text{min}} A_{\text{eff}} t / \sqrt{N_b} \geq M_s$  (see, e.g., [1,2]). The background counts ( $N_b$ ) due to electronic and hadronic (cosmic protons and helium nucleids) cosmic ray showers have been estimated using the following expressions [1]:  $N_e = 3 \times 10^{-2} E_{\text{th}}^{-2.3} t A_{\text{eff}} \Delta\Omega$ ,  $N_h = 6.1 \times 10^{-3} E_{\text{th}}^{-1.7} t A_{\text{eff}} \Delta\Omega$ . As an additional background, one has to consider also the contamination due to isolated muons which depending on the field of view and altitude location of the telescope may be even the dominant background at some energy range (the “muon wall”). Preliminary studies [29] show that

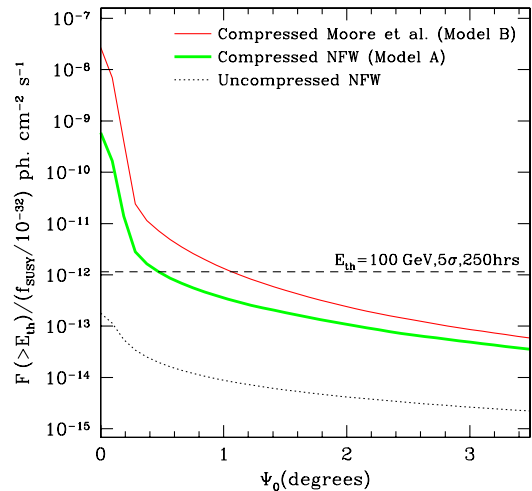


FIG. 3 (color online). Predicted continuum  $\gamma$  fluxes as a function of distance  $\Psi_0$  from the galactic center. The dashed line give the minimum detectable gamma flux  $F_{\text{min}}$  (see text).

the muon background could be as relevant as the hadronic background at  $E_{\text{th}} \gtrsim 100$  GeV while it can be effectively rejected at lower  $E_{\text{th}}$ . The diffuse galactic and extragalactic gamma radiation are negligible compare to this background. The  $E_{\text{th}}$  of an IACT depends on the zenith angle of observation. The galactic center is visible at different zenith angles by all present IACTs (e.g., CANGAROO-III, HESS, MAGIC, VERITAS), but in the best case an  $E_{\text{th}}$  of about 100 GeV can be achieved. The  $A_{\text{eff}}$  is also sensible to the zenith angle of observation, here we choose a value of  $1 \times 10^9$  cm<sup>2</sup>. This detectability condition will allow us to compute the  $5\sigma$  minimum detectable flux  $F_{\text{min}}$  in 250 h of integration with a typical IACT of  $A_{\text{eff}} = 1 \times 10^9$  cm<sup>2</sup> and  $E_{\text{th}} = 100$  GeV (dashed line in Fig. 3). At a given distance from the galactic center only the flux values, for a particular model of the Milky Way, greater than  $F_{\text{min}}$  will be detected. The detection will be much harder and may result only in a central spot in the case of an IACT with higher  $E_{\text{th}}$ , as the  $f_{\text{SUSY}}$  parameter decreases with  $E_{\text{th}}$  (see Fig. 2). For an  $E_{\text{th}} = 100$  GeV the  $f_{\text{SUSY}}/10^{-32}$  factor varies from  $6 \times 10^{-4}$  to 5, approximately.

The compressed MW models presented here likely would result in a detection of the annihilation signal for the discussed SUSY scenario. For the discussed IACTs and exposure times, this detection will be successful only for the very central regions, less than  $\sim 0.4^\circ$ . The uncompressed NFW DM profile of the Model A will not be detected even in the direction of the galactic center. The effect of the adiabatic compression, which was previously ignored, is a crucial factor: in the central  $\sim 3$  kpc of the Milky Way, where the baryons dominate, it does not make sense to use the dark matter profiles provided by cosmological  $N$ -body simulations: the DM must fall into the deep potential well created by the collapsed baryons. Thus, the models presented here are not extreme: they are the starting point for realistic predictions of the annihilation fluxes. One can envision few mechanisms to reduce the effect of the compression. Transfer of the angular momentum to the dark matter as suggested in [23] is an option. Yet, recent simulations of formation of bars indicate that it is difficult to arrange a significant transfer of the angular momentum to the dark matter. The DM density in the central few parsec can be reduced if the central black hole formed by spiraling and merging of two black holes [30]. It can also be changed (probably reduced) by scattering of DM particles by stars in the central 2 pc [31]. If this happens, the flux from the central 2 pc can be significantly reduced. Yet, it will only decrease the amplitude of the central spike. The signal from  $0.4^\circ$  still could be detected because it mostly comes from distances 30–50 pc, which are much less affected by the uncertain physics around the black hole.

We acknowledge support of NASA and NSF grants to NMSU. We thank J. Primack, O. Gnedin, J. Betancort, A. Tasitsiomi, and W. Wittek for discussions.

- [1] L. Bergström, P. Ullio, and J.H. Buckley, *Astropart. Phys.* **9**, 137 (1998).
- [2] A. Tasitsiomi, and A.V. Olinto, *Phys. Rev. D* **66**, 83006 (2002).
- [3] F. Stoehr, S.D.M. White, V. Springel, G. Tormen, and N. Yoshida, *Mon. Not. R. Astron. Soc.* **345**, 1313 (2003).
- [4] G. Jungman, M. Kamionkowski, and K. Griest, *Phys. Rep.* **267**, 195 (1996).
- [5] S. Weinberg, *Phys. Rev. D* **26**, 287 (1982).
- [6] L. J. Hall and M. Suzuki, *Nucl. Phys.* **B231**, 419 (1984).
- [7] J. Edsjo, M. Schelke, P. Ullio, and P. Gondolo, *J. Cosmol. Astropart. Phys.* **04**, 001 (2003).
- [8] D.N. Spergel *et al.*, *Astrophys. J. Suppl. Ser.* **148**, 175 (2003).
- [9] Particle Data Group, K. Hagiwara *et al.*, *Phys. Rev. D* **66**, 10001 (2002).
- [10] C. Calcáneo-Roldán and B. Moore, *Phys. Rev. D* **62**, 123005 (2000).
- [11] P. Ullio, L. Bergström, J. Edsjö, and C. Lacey, *Phys. Rev. D* **66**, 123502 (2002).
- [12] N.W. Evans, F. Ferrer, and S. Sarkar, *Phys. Rev. D* **69**, 123501 (2004).
- [13] J. F. Navarro, C. S. Frenk, and S. D. M. White, *Astrophys. J.* **490**, 493 (1997).
- [14] B. Moore, F. Governato, T. Quinn, J. Stadel, and G. Lake, *Astrophys. J. Lett.* **499**, L5 (1998).
- [15] F. Stoehr, astro-ph/0403077.
- [16] J. Diemand, B. Moore, and J. Stadel, *Mon. Not. R. Astron. Soc.* **353**, 624 (2004).
- [17] P. Colin, A. Klypin, O. Valenzuela, and S. Gottlober, astro-ph/0308348.
- [18] O. J. Eggen, D. Lynden-Bell, and A. R. Sandage, *Astrophys. J.* **136**, 748 (1962).
- [19] Ya. B. Zeldovich, A. A. Klypin, M. Yu. Khlopov, and V. M. Chechetkin, *Sov. J. Nucl. Phys.* **31**, 664 (1980).
- [20] G. R. Blumenthal, S. M. Faber, R. Flores and J. R. Primack, *Astrophys. J.* **301**, 27 (1986).
- [21] R. Jesseit, N. Thorsten, and A. Burkert, *Astrophys. J. Lett.* **571**, L89 (2002).
- [22] O. Gnedin, A.V. Kravtsov, A. Klypin, and D. Nagai, astro-ph/0406247.
- [23] A. Klypin, H. Zhao, and R. S. Somerville, *Astrophys. J.* **573**, 597 (2002).
- [24] J. Binney and N.W. Evans, *Mon. Not. R. Astron. Soc.* **327**, L27 (2001).
- [25] C. Afonso *et al.*, *Astron. Astrophys.* **404**, 145 (2003); P. Popowski *et al.*, astro-ph/0304464.
- [26] P. Gondolo *et al.*, astro-ph/0211238.
- [27] J. Ellis, K. A. Olive, Y. Santoso, and V.C. Spanos, *Phys. Lett. B* **565**, 176 (2003).
- [28] A. Klypin, A.V. Kravtsov, O. Valenzuela, and F. Prada, *Astrophys. J.* **522**, 82 (1999).
- [29] M. Martínez *et al.* (to be published).
- [30] P. Ullio, H. S. Zhao, and M. Kamionkowski, *Phys. Rev. D* **64**, 043504 (2001).
- [31] O. Gnedin and J. Primack, *Phys. Rev. Lett.* **93**, 061302 (2004).